International Journal of Nanomedicine

Dovepress
open access to scientific and medical research

Open Access Full Text Article

ORIGINAL RESEARCH

A Ternary Synergistic eNOS Gene Delivery System Based on Calcium Ion and L-Arginine for Accelerating Angiogenesis by Maximizing NO Production

Guiming Zhang[1,*], Shangcong Han[2,*], Lisheng Wang[3], Yu Yao[1], Kai Chen[4], Si Chen[5]

[1]Department of Urology, The Affiliated Hospital of Qingdao University, Qingdao, 266003, People's Republic of China; [2]Department of Pharmaceutics, School of Pharmacy, Qingdao University, Qingdao, 266021, People's Republic of China; [3]Department of Molecular Diagnosis and Regenerative Medicine, Medical Research Center, The Affiliated Hospital of Qingdao University, Qingdao, 266003, People's Republic of China; [4]Department of Clinical Research, Characteristic Medical Center of Chinese People's Armed Police Force, Tianjin, 300162, People's Republic of China; [5]Department of Anesthesiology, the 991th Hospital of PLA, Xiangyang, 441000, People's Republic of China

*These authors contributed equally to this work

Correspondence: Guiming Zhang, Department of Urology, The Affiliated Hospital of Qingdao University, Qingdao, 266003, People's Republic of China, Email zhangguiming9@126.com

Purpose: This study aimed to construct a delivery system based on L-arginine-modified calcium phosphate (CaP) to load eNOS plasmids (peNOS), which could amply nitric oxide (NO) to repair endothelial damage, promote angiogenic activities and alleviate inflammation.

Methods: pDNA-loaded CaP nanocomplex (CaP/pDNA) were prepared by co-precipitation method, subsequently modified by L-arginine. The gene transfection efficiency, pro-angiogenic and anti-inflammatory ability were investigated in vivo and in vitro. The therapeutic effect on ischemic hindlimb in vivo was assessed.

Results: L-arginine modification augmented the transfection efficiency of CaP/peNOS to elevate the eNOS expression, and then served as NO substrate catalyzed by eNOS. At the same time, calcium ions produced by degradation of CaP carriers enhanced the activity of eNOS. In vitro experiments, the loading capability and transfection performance of R(L)-CaP were confirmed to be superior to that of CaP. Additionally, HUVECs treated with R(L)-CaP/peNOS showed the strongest NO release, cell migration, tube formation and the lowest inflammatory levels compared to the CaP/peNOS and R(D)-CaP/peNOS groups. We also demonstrated the advantages of R(L)-CaP/peNOS in increasing blood reperfusion in hindlimb ischemia mice by accelerating angiogenesis and reducing inflammation, which can be attributed to the highest eNOS-derived NO production.

Conclusion: The combination strategy of peNOS transfection, L-arginine supplement and calcium ions addition is a promising therapeutic approach for certain vascular diseases, based on the synergistic NO production.

Keywords: gene delivery, nitric oxide, L-arginine, calcium ion, angiogenesis

Introduction

Endothelial dysfunction can trigger and exacerbate a variety of vascular diseases, such as atherosclerosis.[1,2] Atherosclerotic plaques in lower extremity arteries tend to lead to inadequate distal blood supply and, in severe cases, to critical limb ischemia (CLI).[3,4] Accelerating vascular endothelial cells (VECs)-dominant vascular regeneration and alleviating excessive inflammation in affected extremities are effective approaches for the treatment of CLI.[5] Normal VECs regulate vascular tone and maintain vascular functions by acting as a physical barrier and secreting vasodilatory substances, anticoagulants, anti-inflammatory cytokines, and many other active components. As a multifunctional gas signaling molecule released by VECs, nitric oxide (NO) was originally identified as a vasodilator and has been shown to inhibit platelet adhesion and smooth muscle cells (SMCs) proliferation, promote VECs morphogenesis, and reduce inflammatory response.[6] The decrease in NO bioavailability is considered as one of the most important causes of endothelial dysfunction.[7] Hence, a moderate increase in NO levels produced

Received: 25 February 2022
Accepted: 27 April 2022
Published: 2 May 2022

by VECs and their bioavailability is of vital significance in mitigating CLI processes through repairing endothelial damage, enhancing VECs angiogenic activities and reducing pro-inflammatory cytokines.[8,9]

Administration of exogenous NO donors can successfully up-regulate intracellular NO levels; however, existing NO donors suffer from deficiencies including disappointing drug release performance, poor bioavailability, and unignored side effects.[10,11] Thoroughly understanding the synthesis mechanism of endogenous NO is valuable for artificially up-regulating its production.[12] Undoubtedly, NO in VECs is generally produced by endothelial nitric oxide synthase (eNOS) catalyzing L-arginine. A growing body of researches is devoted to promoting the release of endogenous NO. Gene therapy is effective to continuously boost NO production through overexpressing eNOS protein, including viral and non-viral transfection to transport eNOS plasmids (peNOS), VEGF plasmids (pVEGF), and ZNF580 plasmids (pZNF580), etc. In addition, as the substrate for eNOS, L-arginine promotes NO production in a dose-dependent manner. Kohli et al facilitated NO release and restoration of VECs function via supplementing L-arginine by oral intake in the treatment of diabetes.[13] It has been demonstrated that generated endogenous NO can decrease intracellular free calcium ion levels, which favors vasodilation.[14] Interestingly, literature suggested that maintenance of cytosolic calcium ion level plays important roles in enhancing the effectiveness of L-arginine.[15] Recently, elevating the concentration of extracellular calcium ion was confirmed to promote NO production via enhancing intracellular calcium ion concentration and Ca^{2+}-sensing receptor (CaSR) and Gq/11 protein-mediated the activity of eNOS.[16]

Effective therapeutic genes and efficient gene carriers are essential for gene therapy. Although delivery of peNOS, pVEGF and pZNF580, etc can elevate the release of endogenous NO, peNOS are the most direct and attractive option.[17] As for gene carrier, non-viral nanocarriers hold great promise for their low immunogenicity and less expensive compared to viral carriers.[18] Nowadays, inorganic nanoparticles for gene delivery such as silica, calcium phosphate (CaP), and magnetite developed rapidly due to their outstanding stability, cost-effective and ease of preparation. CaP is a promising transfection agent as it is an important component of tissues such as bones and teeth and can be progressively degraded by the acidic environment in the endo/lysosomes and release plasmid DNA (pDNA) upon completion of pDNA loading and cellular uptake.[19,20] Co-precipitation is the simplest and most classical method for the preparation of CaP/pDNA nanocomplexes, including preparation in the aqueous-phase or microemulsion.[21] There are many processes to prepare CaP/pDNA nanocomplexes. Adding a pre-mixed mixture of calcium ions and pDNA to a phosphate buffer solution to produce different forms of CaP/DNA nanocomplexes by controlling the molar ratio of calcium to phosphorus, which is the most typical strategy.[22] The resulting CaP is filtered through a membrane and then incubated with pDNA to adsorb it outside the CaP nucleus to obtain a more uniform nanocomplexes.[23] Moreover, CaP/pDNA nanoparticles with a multilayer structure can be prepared by layer-by-layer assembly, ie, CaP is first prepared and then added to the pDNA solution, and the process is repeated to form nanoparticles with a multilayer structure, which improved the transfection efficiency of the pDNA.[19] However, the transfection efficiency of CaP is still inferior to the commercialized cationic liposomes and polymers. To improve the transfection performance, one or more CaP coating, PEG, PEI, protamine, etc., were used for the surface modification of CaP-loaded plasmid DNA (CaP/pDNA) nanocomplexes.[24–26]

In this work, we are committed to enlarge eNOS-derived NO production to promote angiogenesis related activities of VECs and reduce the inflammatory response, ultimately relieving CLI by re-building collateral vascular circulation and normalizing the microenvironment. In order to maximize NO output, a "one-stone-three-birds" strategy has been devised (Figure 1). That is, we developed a bioactive carrier based on calcium ions and L-arginine to deliver peNOS, in which calcium ions and L-arginine not only act as carriers to condense pDNA and improve transfection efficiency, but also transform their identities into the enhancers of eNOS activity for further elevating NO production after completion of the delivery task.[27] The positive feedback between overexpressed eNOS, and calcium ions and L-arginine degraded from CaP was built to synergistically promote NO production. In vitro experiments first demonstrated the role of L-arginine in enhancing loading ability and transfection efficiency of CaP as a gene carrier. Subsequently, the effect of the ternary peNOS delivery system in synergistically boosting NO release was identified by measuring the nitrate level in media. In vitro angiogenesis-related activities, and inflammatory levels of VECs confirmed the advantages of synergistic NO release. Finally, we verified that the triple peNOS delivery system contributes to the restoration of perfusion and normalization of the microenvironment in an CLI model. In a word, the combination of calcium ions, L-arginine and

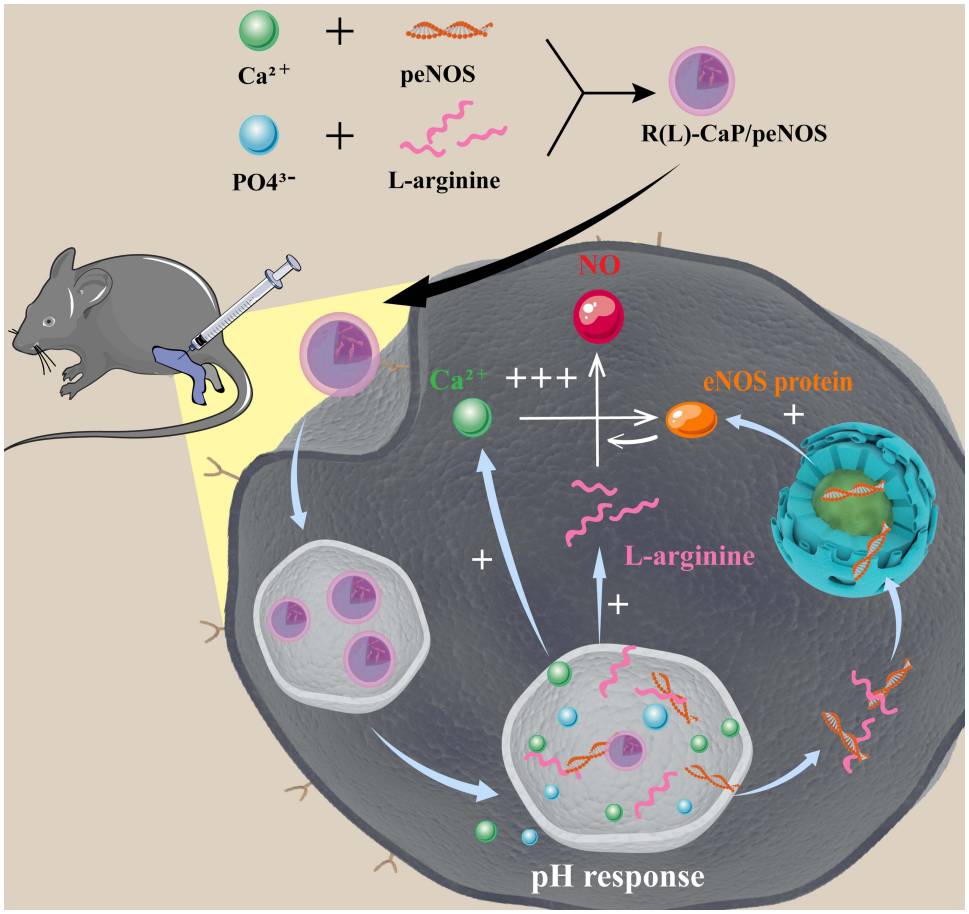

Figure 1 Schematic diagram illustrating the preparation of R(L)-CaP/peNOS nanocomplexes based on calcium ion and L-arginine and their intracellular transport in VECs for synergistic NO production.

peNOS fully amplified the eNOS-derived NO production from multiple pathways, thereby exerting enhanced pro-vascularization and anti-inflammatory effects.

Experimental Section

Materials

The materials were provided in Supporting Information (SI).

Preparation of Nanocomplexes

pDNA-loaded calcium phosphate nanocomplex (CaP/pDNA) were prepared by typical co-precipitation method. Different masses of pDNA (8.3 μg, 4.2 μg, 2.8 μg, 2 μg, 1.7 μg) were added drop by drop to $CaCl_2$ solution (150 μL, 250 mM) and incubated for 20 min at room temperature to form solution A. Subsequently, Na_2HPO_4 solution (150 μL, 3 mM) was added slowly dropwise to solution A under stirring conditions. Due to the strong tendency to precipitation of CaP, CaP/pDNA nanocomplexes at different weight ratio of $CaCl_2$ and pDNA (500/1, 1000/1, 1500/1, 2000/1, 2500/1) were prepared with the rapid formation of nanoparticles, respectively. In addition, in order to prepare L-arginine-modified CaP/pDNA, ie, R(L)-CaP/pDNA, L-arginine was dissolved in deionized water up to concentrations of 3% firstly. Then, a mixture of L-arginine solution (75 μL) and Na_2HPO_4 solution (75 μL, 6 mM) was added to solution A (150 μL) to obtain R(L)-CaP/pDNA nanocomplexes. Similarly, R(D)-CaP/pDNA nanocomplexes were obtained by replacing L-arginine with D-arginine following the procedure for the preparation of R(L)-CaP/pDNA.

Characterization of Nanocomplexes

Agarose gel electrophoresis was conducted to assess the loading capability of different gene carriers for pDNA (5.3 kp). 1 kb DNA ladder was used as a marker. The procedure was shown in SI. In addition, carriers/pDNA at different mass ratios were freshly prepared and tested for their average diameter and zeta potential by Zetasizer Nano ZS. The morphology of R(L)-CaP/peNOS was detected by transmission electron microscope (TEM).

Cytotoxicity of Gene Complexes

Cytotoxicity is important for transfection reagents. Cell Counting Kit-8 (CCK-8) assay was performed to evaluate the cytotoxicity of various gene complexes. Human umbilical vein endothelial cells (HUVECs) were seeded into 96-well plates overnight and starved with serum-free DMEM for 12 h. Then, different concentration gradients of CaP/pEGFP (plasmids coding enhanced green fluorescent protein are denoted as pEGFP), R(L)-CaP/pEGFP and R(D)-CaP/pEGFP nanocomplexes (50, 100, 150, 200, 300 μM, calculated based on $PO4^{3-}$) were added to the medium for 4 h, respectively, and then replaced with fresh complete medium for a further 20 h. Phosphate buffered saline (PBS,10 mM, pH=7.2–7.4) -treated HUVECs were served as control. Discarding all medium and adding serum-free DMEM containing 10% CCK-8 reagent to co-culture with cells for 2 h. Multifunctional microplate reader was used to measure the absorbance at 450 nm to reflect the cell viability. The relative cell viability is the cell viability of the gene complex-treated groups relative to that of the PBS-treated group.

Flow Cytometric Assay

Flow cytometry was performed to determine the cellular uptake of gene complexes. HUVECs were seeded in 6-well plates and collected in after the transfection with Cy5 labeled peNOS (denoted as Cy5-peNOS) at a concentration of $PO4^{3-}$ of 150 μM for 4 h. After washing 3 times with PBS (10 mM, pH=7.2–7.4), the cells were resuspended to a density of 1×10^6 cells/mL. Subsequently, cellular fluorescence was detected and counted by flow cytometry.

Intracellular Trafficking Observed by Confocal Laser Scanning Microscope (CLSM)

HUVECs were seeded in confocal dishes and transfected with gene complexes containing Cy5-peNOS at a concentration of $PO4^{3-}$ of 150 μM, which emits a red fluorescence. After 4 h of transfection, the medium was replaced with fresh complete medium and incubation continued for another 20 h. Afterwards, the LysoTracker (green fluorescence) and Hoechst33342 (blue fluorescence) were used to stain endo/lysosome and cell nucleus, respectively. Thereupon, the subcellular location of peNOS was observed by CLSM, ie, pDNA in endo/lysosome appeared as yellow spots, and pDNA in nucleus was pink spots.

In vitro Gene Expression

Green fluorescence protein (GFP) and eNOS mRNA expression can reflect the transfection efficiency of gene carriers in vitro at the protein and mRNA levels, respectively. HUVECs overexpressed green fluorescence protein was directly observed by the inverted fluorescence microscope after 24 h of transfection with nanocomplexes containing pEGFP at a concentration of $PO4^{3-}$ of 150 μM. Furthermore, HUVECs were seeded in 6-well plate and transfected with different gene complexes loaded with peNOS for 24 h. Then, the quantitative real-time polymerase chain reaction (PCR) assay was carried out to characterize the mRNA level of eNOS. The detailed description was given in SI.

Intracellular NO Level

The amount of NO released by HUVECs was determined by detecting intracellular NO levels by 3-Amino,4-amino-methyl-2',7'-difluorescein, diacetate (DAF-FM DA). HUVECs were spread in 96-well plates. CaP, R(L)-CaP, R(D)-CaP and their gene complexes with peNOS (at a concentration of $PO4^{3-}$ of 150 μM) were added into the media and incubated for 24 h. DAF-FM DA was diluted with fresh medium (without serum and phenol red) at a ratio of 1:1000 to a final concentration of 5 μM. The original medium was replaced with DAFM DA-containing medium (50 μL per well) and incubation was continued for 20 min in the incubator. After sufficient washing with PBS, the fluorescence values were

tested at 495 nm excitation wavelength and 515 nm emission wavelength using multifunctional microplate reader to reflect intracellular NO level.

Cell Supernatant Assay

HUVECs were spread into 6-well plates and incubated overnight. LPS was added into the serum-free DMEM (the final concentration of LPS was 1 μg/mL) for 12 h to active HUVECs. Then, CaP, R(L)-CaP, R(D)-CaP and their gene complexes with peNOS (at a concentration of $PO4^{3-}$ of 150 μM) were added into the media and incubated for 4 h. Cells were continued to be cultured for 20 h with complete DMEM. At time point of 24 h of transfection, the supernatant in 6-well plates was extracted and used to perform enzyme-linked immunosorbent assay (ELISA). The concentration of inflammatory cytokines (IL-6, TNF-α) was obtained according to the manufacturer's instructions of ELISA.

Angiogenesis-Related Activities

The angiogenic properties of HUVECs after transfection with different gene complexes were assessed via Transwell assay and tube formation assay in vitro. In brief, HUVECs were seeded in 6-well plates at a density of 2×10^5 cell/well. After transfection for 24 h of various peNOS nanocomplexes at a concentration of $PO4^{3-}$ of 150 μM, cells were digested by trypsin and collected after centrifugation. Next, use serum-free DMEM to resuspend the enriched cells to a density of 4×10^5 cell/mL. DMEM containing 10% FBS (1 mL) was added to the lower chamber of the Transwell (8 μm), which was placed in the 24-well plates. Then, 100 μL cell suspension was added into the upper chamber and incubation was continued for 6 h. Finally, images of cells migrated through the Transwell membrane are acquired by microscopy after fixation and staining. For tube formation assay, Matrigel was pre-layered in 96-well plate (60 μL/well). After solidification of the Matrixgel, 100 μL of abovementioned cell suspension was added to each well (4×10^4 cell/well) and incubated at 37°C under 5% CO_2 for 6 h. The images of the tube formation were obtained by microscopy.

In vivo Hindlimb Ischemia Model

The hindlimb ischemia model was established in the BALB/c (male, 7 weeks, 20 g) by ligating the femoral artery in the right limb. After surgery, various gene complexes (containing 5 μg peNOS) are injected into the gastrocnemius muscle of the ischemic limb at multiple points (3 injection sites evenly distributed), with a frequency of 3 days per injection. Blood perfusion in the limb was acquired by laser Doppler flowmetry on postoperative days 0, 7 and 14. The perfusion ratio of the ischemic limb to the normal limb in the same mouse is used to indicate the degree of ischemia. On day 14, the gastrocnemius muscles of the left legs were obtained and performed hematoxylin and eosin (H&E) staining, and immunofluorescence staining for monoclonal antibodies against CD31 (anti-CD31) and monoclonal antibodies against F4/80 (anti-F4/80) to mark ECs and macrophages, respectively. The detailed operation can be found in the SI. All animal experiments were performed and approved by the "Guide for the protection and use of experimental animals" of the American National Institutes of Health.

Statistical Analysis

All data were expressed as mean ± standard deviation (SD). Significant difference was counted by Student's *t*-test.

Results and Discussion

Preparation and Characterization of Nanoparticles

CaP, R(L)-CaP and R(D)-CaP and their nanocomplexes loaded with pDNA were prepared based on the co-precipitation of calcium ions and phosphate ions. Following the rapid formation of CaP and CaP@pDNA nanoparticles, L-arginine and D-arginine were introduced to the nanoparticles by electrostatic and hydrogen bonding between guanidine group in arginine and phosphate in order to improve the transfection properties.[28] Agarose gel electrophoresis assay was used to analyze the immobilization effect of various nanocarriers with pDNA. Figure 2A–C illustrated that CaP are robust enough to immobilize pDNA when the weight ratio of $CaCl_2$ to pDNA ≥1500, while R(L)-CaP and R(D)-CaP can totally prevent pDNA migration when w/w of $CaCl_2$/pDNA was 1000. That is, R(L)-CaP and R(D)-CaP exhibit stronger pDNA

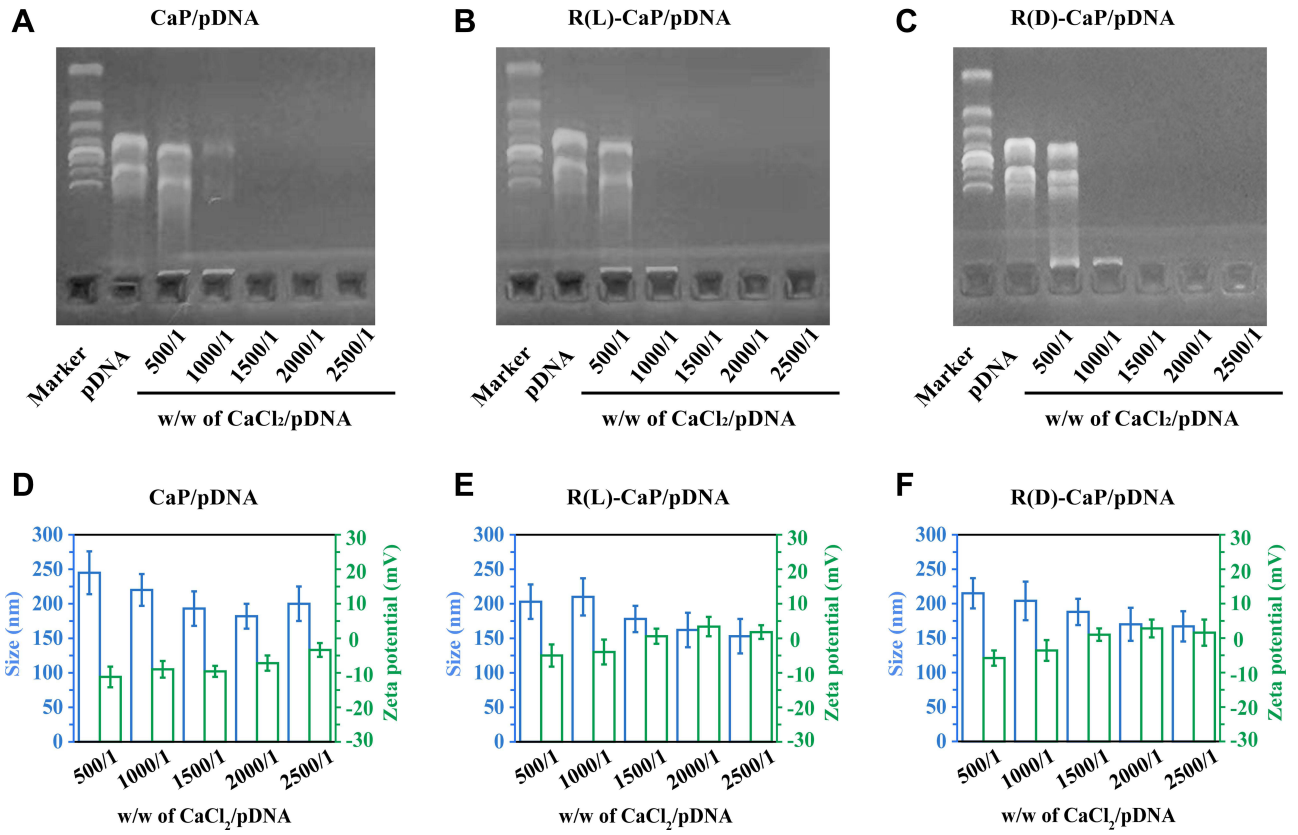

Figure 2 Graphics of agarose gel retardation (**A**–**C**) and particle size and zeta potential (**D**–**F**) of different gene complexes with weight ratios of $CaCl_2$ and pDNA from 500/1 to 2500/1.

loading ability than CaP, which might be attributed to the binding of guanidine group in L-arginine and D-arginine to the phosphate group in pDNA.[29] As key characteristic for transfection performance, particle size and zeta potential of freshly prepared gene complexes at different weight ratios were investigated. As shown in Figure 2D–F, at a weight ratio of 500/1 for $CaCl_2$/pDNA, the size of the nanocomplexes formed is on the large side because pDNA is not fully condensed by carriers. As the weight ration of $CaCl_2$ to pDNA increases, the particle size of the nanoparticles gradually stabilizes at around 200 nm. At the same weight ratio of $CaCl_2$ to pDNA, R(L)-CaP/pDNA and R(D)-CaP/pdna displayed a smaller particle size compared to CaP/pDNA. The reduction in particle size may be related to the condensation of pDNA by L-arginine and D-arginine in R(L)-CaP/pDNA and R(D)-CaP/pDNA. All measured CaP/pDNA nanocomplexes showed slightly negative charge, and rises to close to neutrality with increasing of the weight ratio of $CaCl_2$ to pDNA (Figure 2D). The modification of L-arginine or D-arginine on nanoparticles resulted in an increase in zeta potential compared to CaP/pDNA. The high positive charge density allowing for tighter binding of the pDNA. As for the R(L)-CaP/pDNA and R(D)-CaP/pDNA nanocomplexes, the zeta potential gradually became positive with a gradual increase in the weight ratio of $CaCl_2$ to pDNA. The morphology of R(L)-CaP/pDNA was shown in the Supplementary Materials. The weight ratio of 2000/1 for $CaCl_2$/pDNA was chosen for the subsequent bio-characterization owing to the suitable size and zeta potential of nanocomplexes at this ratio, which facilitates cellular uptake.

In vitro Transfection Performance

A critical characteristic of gene delivery system is cytocompatibility. HUVECs exposed to different concentrations of nanocomplexes for 6 h and continue to culture for another 18 h with complete DMEM, followed by the relative cell viability was determined by CCK-8 assay. HUVECs treated with PBS were served as control. As shown in Figure 3A, all nanocomplexes maintained low cytotoxicity over the concentration range tested, ie, the relative cell viability of HUVECs co-incubated with nanocomplexes exceeded 70% in the final concentration range from 50 to 300 μM (calculated based on

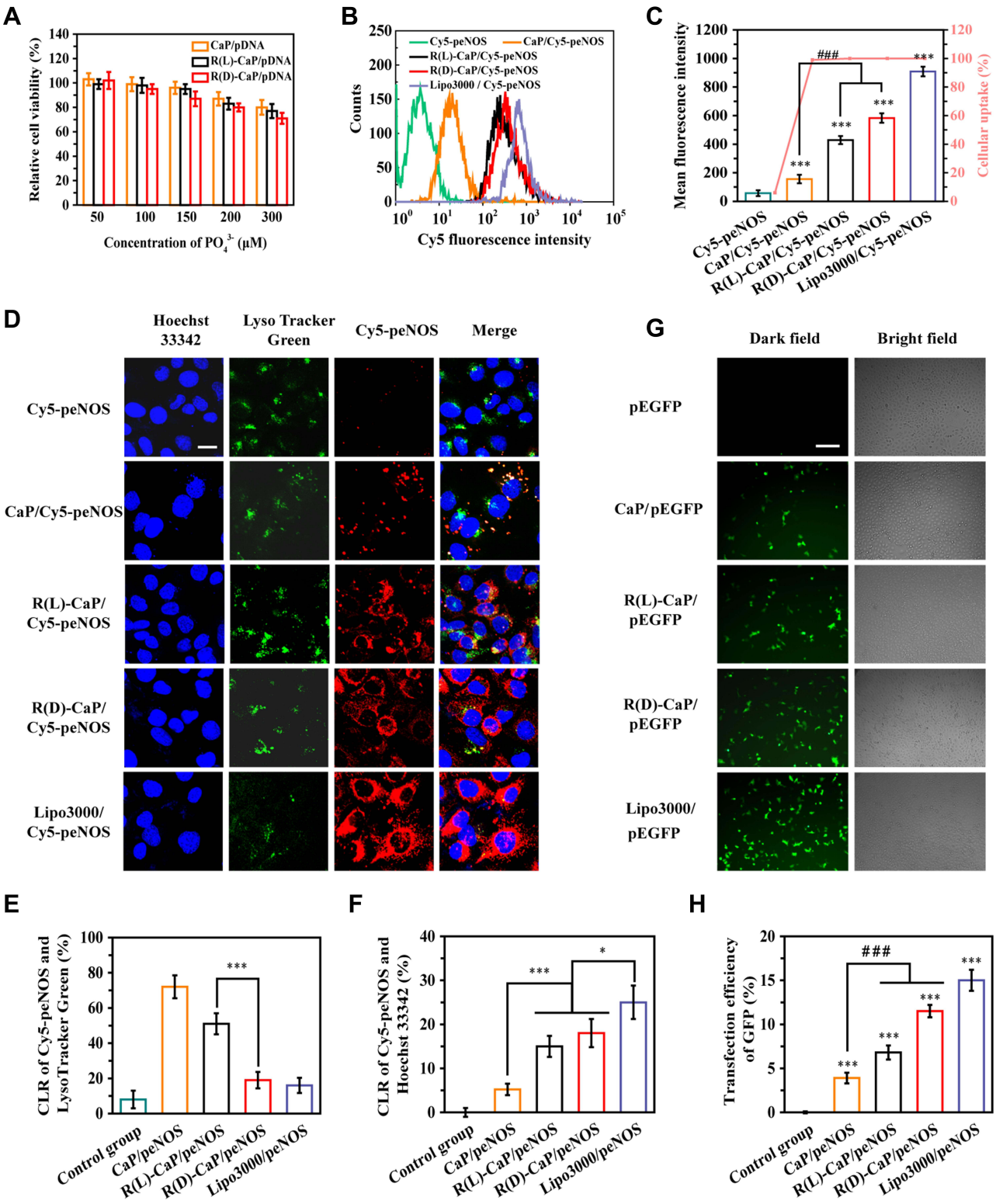

Figure 3 Transfection properties of various gene complexes. (**A**) The relative cell viability of HUVECs incubated with CaP/pEGFP, R(L)-CaP/pEGFP and R(D)-CaP/pEGFP for 24 h. The results of (**B**) cellular uptake, (**C**) mean fluorescence intensities and (**D**) subcellular location of gene complexes with Cy5 labelled peNOS. The scale bar is 20 μm. (**E**) The quantitative results of (**F**) CLR of Cy5-peNOS and LysoTracker Green, (**F**) CLR of Cy5-peNOS and Hoechst 33342 to reflect the localization rate of target genes in endo/lysosomes and nucleus, respectively. (**G**) The representative images and (**H**) quantitative results of transfection efficiency of different gene carriers was evaluated after 24 h of transporting pEGFP. The scale bar is 100 μm. mean ± SD, n = 3, *P <0.05, ***P < 0.001, $^{###}$P < 0.001.

corresponding PO_4^{3-} molar concentration). Additionally, all nanocomplexes induced a dose-dependent cytotoxicity. R(L)-CaP/peEGFP showed slightly less cytotoxicity towards HUVECs compared to R(D)-CaP/pEGFP at the same concentration, probably due to the unnatural D-arginine residues in R(D)-CaP/peEGFP. Overall, the cytotoxicity of nanocomplexes at the transfection dose (a final PO_4^{3-} molar concentration is 150 μM) is negligible.

To investigate the cellular uptake of different gene complexes, HUVECs were treated with nanocomplexes containing Cy5 fluorescein-labelled peNOS (Cy5-peNOS) and incubated for 6 h. Naked Cy5-peNOS and lipo3000/Cy5-peNOS-treated cells were used as negative control and positive control, respectively. After detecting the intracellular fluorescence by flow cytometry, almost no fluorescent signal was inspected in cells treated with naked Cy5-peNOS (Figure 3B and C). Notably, near 100% cellular uptake was found in HUVECs exposed to gene complexes. As expected, the mean fluorescence intensity (MFI) of R(L)-CaP/Cy5-peNOS and R(D)-CaP/Cy5-peNOS-treated HUVECs significantly higher than that of CaP/Cy5-peNOS. Additionally, cells transfected by R(D)-CaP/Cy5-peNOS exhibited brighter fluorescence than R(L)-CaP/Cy5-peNOS, second only to the lipo3000/Cy5-peNOS group.

Subcellular localization of the target gene is also essential for assessing the transfection performance of gene carriers. After co-incubation with gene complexes for 24 h, HUVECs were stained for endo/lysosomes (appeared green) and nucleus (appeared blue). The subcellular location of Cy5-peNOS (red fluorescence) was tracked by confocal laser scanning microscopy (CLSM) (Figure 3D). Almost no red fluorescence was detected in naked Cy5-peNOS-transfected HUVECs. For CaP/Cy5-peNOS-treated group, only the small amount of red fluorescence appeared in the endo/lysosomes and formed yellow dots. When HUVECs were treated with the R(L)-CaP/Cy5-peNOS and R(D)-CaP/Cy5-peNOS nanocomplexes, the markedly increased red fluorescence than that of CaP/Cy5-peNOS was observed in HUVECs, which is consistent with the results of cellular uptake measured by flow cytometry. The endo/lysosome co-localization ratios (CLR) of R(D)-CaP/Cy5-peNOS were obviously less than that of the R(L)-CaP/Cy5-peNOS, which might be due to that some of R(D)-CaP/Cy5-peNOS enter HUVECs via a direct membrane translocation internalization pathway, rather than the typical endocytosis approach.[27] In addition, the nuclear localization rate of Cy5-peNOS (appeared pink) showed that lipo3000/Cy5-peNOS group possessed the most pink dots, followed by R(L)-CaP/Cy5-peNOS and R(D)-CaP/Cy5-peNOS groups, illustrating that Cy5-peNOS in these groups can escape from endo/lysosomes and achieved higher nucleus accumulation than CaP/Cy5-peNOS group.

The transfection efficiency of gene carriers was investigated by transfecting pEGFP and detecting green fluorescence in HUVECs, which is intuitive and uncomplicated. As presented in Figure 3E, there is a gradual increase in green fluorescence in HUVECs treated with pEGFP, CaP/pEGFP, R(L)-CaP/pEGFP, R(D)-CaP/pEGFP and lipo3000/pEGFP, respectively, which is consistent with cellular uptake and nuclear positioning rate. Excitingly, the aforementioned in vitro studies related to transfection performance revealed that L-arginine and D-arginine modification has a positive effect on the transfection efficiency of CaP. These results were in line with our hypothesis.

In vitro eNOS Expression and NO Production

We used L-arginine to functionalize CaP/pDNA nanocomplexes not only for its ability to improve the loading capacity and transfect efficiency of CaP/pDNA but also for its bioactive function as a substrate. PBS-treated HUVECs were used as the control group. The mRNA expression of eNOS was evaluated to further reflect the transfection efficiency (Figure 4A). As expected, no statistical difference can be observed between the control group and only carriers-treated groups. HUVECs transfected with peNOS nanocomplexes exhibited obviously enhanced eNOS mRNA level compared with the control group, and the trend was consistent with the GFP expression trend. After treating HUVECs for 24 h with various nanoparticles, DAF-FM DA was used to measure the intracellular NO by detecting the cellular fluorescent values. As shown in Figure 4B, R(L)-CaP showed higher nitrate level than control group, probably corroborating the substrate effect of L-arginine. The significantly elevated nitrite levels were found in groups transfected with peNOS. Remarkably, R(L)-CaP/peNOS exhibited moderate transfection efficiency but the most NO production. The lipo3000/peNOS-treated group had approximately twice as much mRNA expression of eNOS as the CaP/peNOS-treated group, but their NO levels had no significant difference, which might be attributed to calcium ions in enhancing eNOS activity.

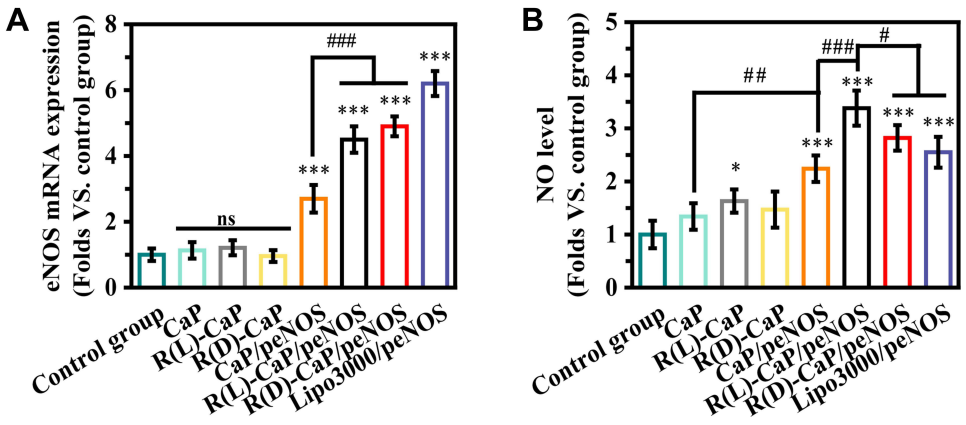

Figure 4 (**A**) eNOS mRNA and (**B**) NO levels were detected in HUVECs after treatment with different nanoparticles. (mean ± SD, n = 3, ns means "no statistical difference". *and $^{\#}P < 0.05$, $^{\#\#}P < 0.01$, ***and $^{\#\#\#}P < 0.001$).

In vitro Pro-Angiogenic and Anti-Inflammatory Efficiency

eNOS-derived NO plays important roles in angiogenesis and inflammation response. Transwell assay was performed to evaluate the migration ability of HUVECs transfected with different gene complexes. Figure 5A and C showed the representative images and statistical data of migrated cells. Cells treated with only peNOS were served as the negative control. Other groups that overexpressed eNOS had increased migrated cells than the peNOS group. Specifically, HUVECs exposed to R(L)-CaP/peNOS possessed the most numbers of migrated cells (403), followed by those transfected by R(D)-CaP/peNOS (322), lipo3000/peNOS (309), and CaP/peNOS (220). More importantly, as shown in Figure 5B and D, HUVECs co-cultured with these gene complexes all promoted the tube formation. We observed a trend in the effect of the these nanocomplexes on tube formation effect consistent with NO production and cell migration. In addition, R(L)-CaP/peNOS-treated cells had the maximum number of lumens.

In order to assess the therapeutic potential of gene complexes on microenvironmental normalization, we measure the levels of representative pro-inflammatory cytokines (IL-6 and TNF-α) by Elisa assay. LPS (1 μg/mL) was added into the media to induce the inflammatory environment. Lower levels of IL-6 and TNF-α were detected in peNOS gene complexes-treated groups compared with the control group (LPS stimulated HUVECs treated with naked peNOS), demonstrating that anti-inflammatory effect of NO. More excitingly, transfection with R(L)-CaP/peNOS maximally alleviated inflammation and reduced IL-6 and TNF-α release, which further verifying the multiple roles played by R(L)-CaP/peNOS nanocomplexes in NO production and the morphogenesis of HUVECs (Figure 5E and F).

The Therapeutic Effect on Ischemic Hindlimb in vivo

To assess the anti-ischemic effect of various gene complexes in vivo, we established a hindlimb ischemic model and intramuscularly injected different nanocomplexes into the ischemic tissue. peNOS, CaP/peNOS, R(L)-CaP/peNOS, R(D)-CaP/peNOS and lipo3000/peNOS with the same dose of peNOS (10 μg per injection). As shown in Figure 6A and C, the blood perfusion of ischemic limb was obviously increased in the gene complexes treatment groups compared with the naked peNOS-treated group, benefiting from the pro-angiogenic effect of enhanced eNOS-derived NO. Of these, the limbs injected with R(L)-CaP/peNOS exhibited the highest levels of blood perfusion. The histopathological analysis was conduct on day 14 for further exploration at the cellular and protein levels. The H&E staining in Figure 6B shows the morphology of the muscle fibers. Significant regular size and shape muscle fibers can be noticed in R(L)-CaP/peNOS and R(D)-CaP/peNOS-treated groups, suggesting a better recovery at tissue level for the two groups. In addition, the R(L)-CaP/peNOS group showed a statistically significant increase in vessel surface density compared to CaP/peNOS and R(D)-CaP/peNOS (Figure 6D). Furthermore, the percentage of F4/80-positive cells indicated the anti-inflammatory ability of these gene complexes in vivo (Figure 6E). All groups overexpressed eNOS groups showed the reduced inflammatory levels. Among them, R(L)-CaP/peNOS nanocomplexes remarkably suppressed the infiltration of inflammatory cells. These results in vivo were generally consistent with the tendency of data in vitro. The improved pro-angiogenic effect

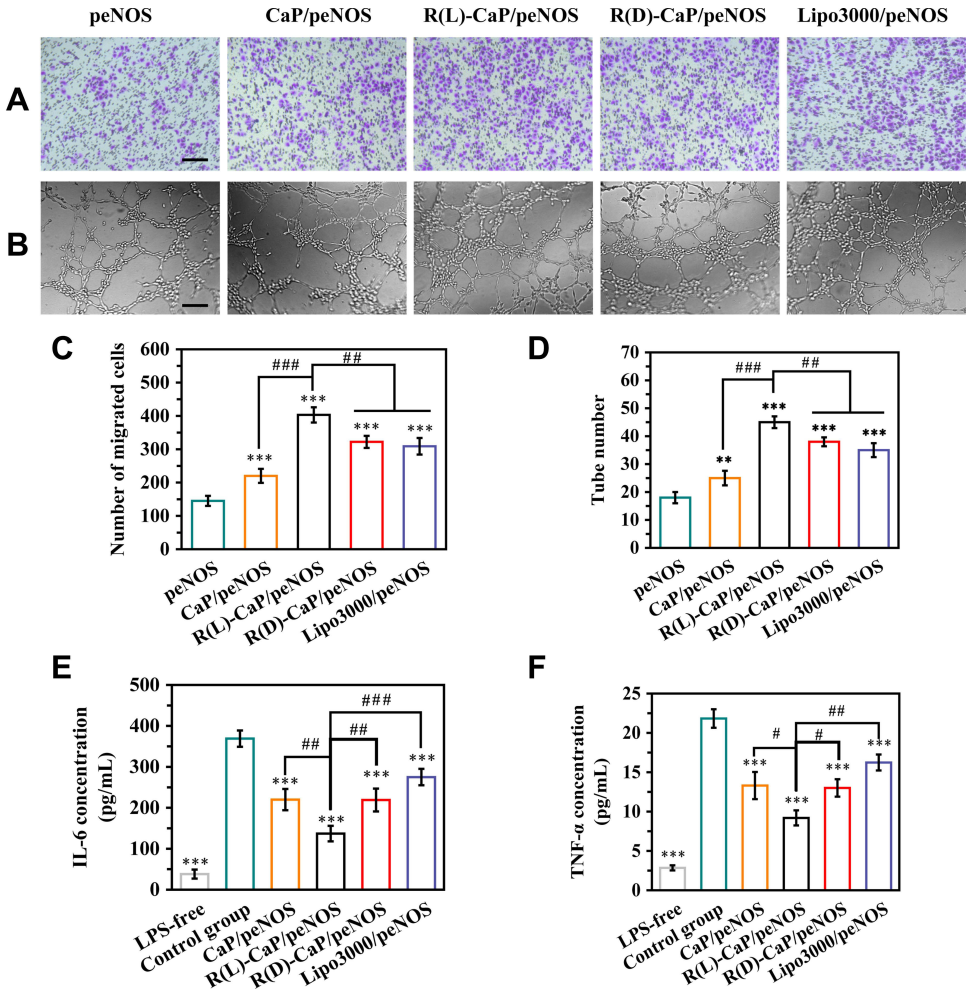

Figure 5 In vitro pro-angiogenic and anti-inflammatory ability of gene complexes. The migration ability of HUVECs treated with various nanocomplexes was evaluated by (**A**) representative images of migrated cells passing through Transwell chamber, and (**C**) the statistical results of the number of migrated cells. (**B**) Representative images of tube formation, and (**D**) the statistical results of tube number, reflecting the tube formation ability of HUVECs treated with various nanocomplexes. The release of (**E**) IL-6 and (**F**) TNF-α in culture media of LPS-unstimulated HUVECs and LPS-stimulated HUVECs after treatment with different gene complexes. The scale bar is 100 μm. mean ± SD, n = 3, $^{\#}P < 0.05$, **and $^{\#\#}P < 0.01$, ***and $^{\#\#\#}P < 0.001$.

and anti-inflammatory effect of R(L)-CaP/peNOS nanocomplexes can be attributed to the synergistically increased NO production caused by elevated L-arginine, calcium ions and eNOS expression.

Discussion

In this study, we constructed a gene delivery system that synergistically produces ECs-derived NO to promote morphogenesis of ECs while reducing inflammation. On the one hand, from the perspective of vector design, CaP was chosen as the core of the delivery system to load pDNA, and L-arginine was modified in the outer layer of the delivery system to enhance its transfection efficiency; on the other hand, both CaP and L-arginine can be transformed into synergists for NO production by eNOS after completing the gene delivery task, ie calcium ions generated from CaP degradation can enhance the activity of eNOS, and L-arginine can act as a substrate for NO production by eNOS, thus forming a ternary synergistic delivery system with peNOS for maximum NO production. In order to verify whether the above delivery system was successfully developed, we explored both its gene transfection efficiency and the synergistic production of bioactive NO, respectively.

We prepared CaP/peNOS nanoparticles and CaP/peNOS coated with L-arginine or D-arginine in the outer layer, ie, R(L)-CaP/peNOS and R(D)-CaP/peNOS, and the commercial transfection reagent loaded with peNOS (lipo3000/peNOS) was used as a positive control. The effect of the outer layer of arginine on the gene loading capacity of the vector was

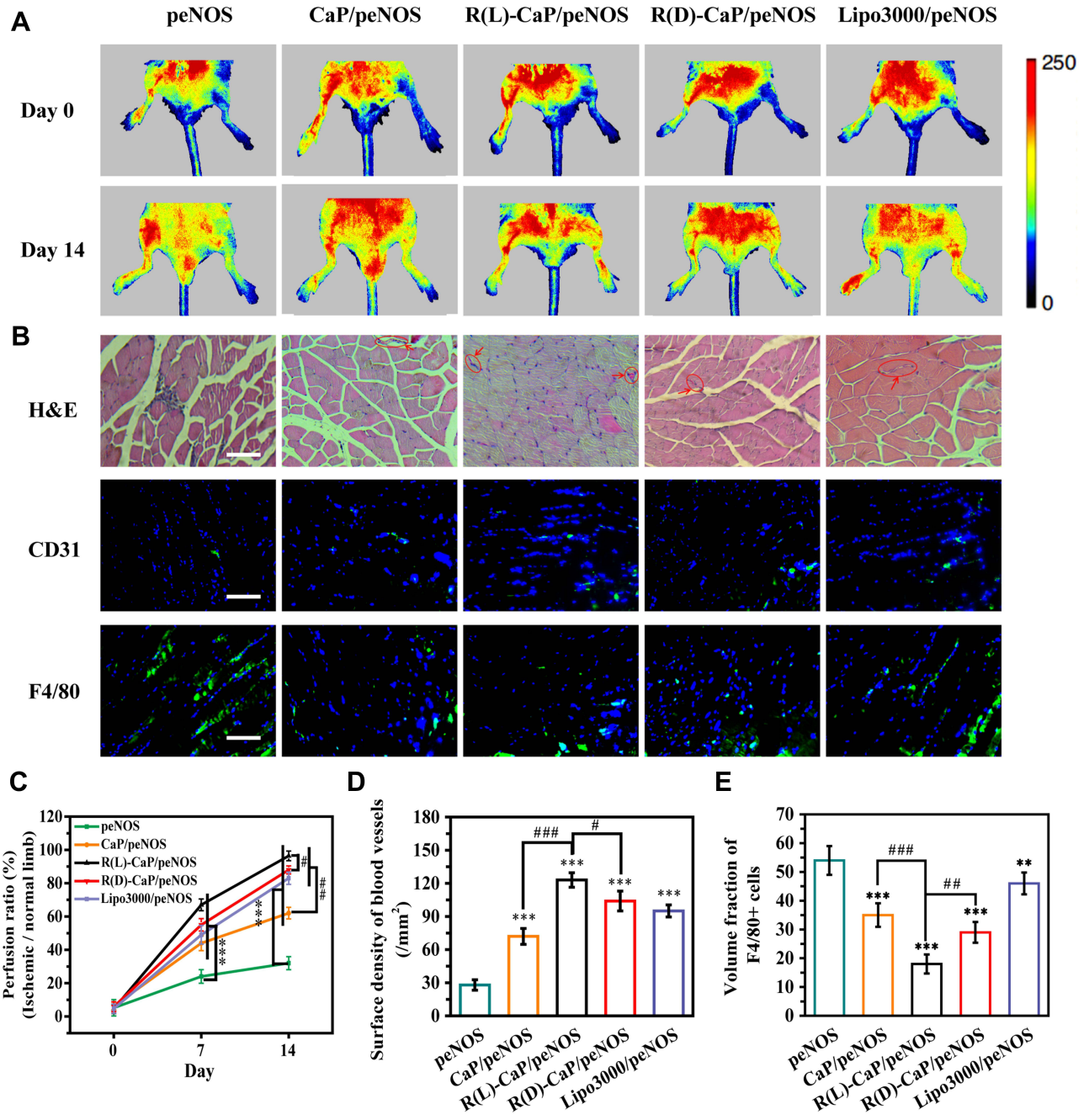

Figure 6 (**A**) Representative images detected by laser Doppler flowmetry and (**C**) their statistical results of blood perfusion of hindlimbs treated with different nanocomplexes. (**B**) Representative images of H&E staining, and investigation of immunofluorescence staining of CD31 and F4/80-positive cells. The scale bar is 100 μm. Statistical results of (**D**) surface density of blood vessels and (**E**) inflammatory levels. Mean ± SD, n = 3. $^{\#}P < 0.05$, **and $^{\#\#}P < 0.01$, ***and $^{\#\#\#}P < 0.001$.

verified by agarose gel electrophoresis assay. The modification of either L-arginine or D-arginine significantly enhanced the immobilization effect of the vector on pDNA, which might be due to the binding of guanidine group in L-arginine and D-arginine to the phosphate group in pDNA (Figure 2A–C). In addition, as shown in Figure 2D–F, the potential of the arginine modified delivery system was obviously increased, which theoretically facilitates the subsequent cellular uptake. Afterwards, this speculation was verified by flow cytometry experiments, and the results were shown in Figure 3C. The MFI of R(L)-CaP/Cy5-peNOS and R(D)-CaP/Cy5-peNOS-treated HUVECs was significantly higher compared to CaP/Cy5-peNOS. CLSM was used to visualize the subcellular localization of the target gene more intuitively (Figure 3D). Higher intracellular fluorescence and the nuclear localization rate can be found in HUVECs

treated with R(L)-CaP/Cy5-peNOS and R(D)-CaP/Cy5-peNOS. These results might be due to their increased positive charge density and the guanidine groups derived from L-arginine and D-arginine. Among them, R(D)-CaP/Cy5-peNOS showed higher fluorescence than R(L)-CaP/Cy5-peNOS, resulting from D-arginine conferring the membrane translocation internalization pathway to gene complexes to enhance its uptake by cells. Most importantly, the expression of GFP visually demonstrates the efficiency of transfection. Transfection fluorograms confirmed that CaP, chosen as the core of the delivery system, can successfully deliver pDNA, while modification with arginine in the outer layer can effectively improve its transfection efficiency (Figure 3E and H). In a series of studies, arginine peptide has been shown the ability to promote the targeting delivery efficacy with practical advantages in transmembrane efficiency. Chang's group constructed L-arginine and L-arginine peptide modified chitosan to deliver plasmids. The results demonstrated that the gene transfection efficiency of chitosan was significantly enhanced after arginine-graft.[30] Based on its positive charge and guanidine structure under physiological conditions, arginine is widely used as a drug and gene carrier.[31]

To confirm the synergistic role of the ternary gene delivery system in bioactive NO production, we assessed the amount of NO released after different treatments and its impact on ECs including angiogenesis-related functions and anti-inflammatory functions. As shown in Figure 4, HUVECs treated with CaP showed higher nitrate level compared to PBS, and R(L)-CaP/peNOS group showed higher nitrate level than CaP/peNOS and R(D)-CaP/peNOS groups, although its transfection efficiency was lower than that of R(D)-CaP/peNOS. These data fully confirm the roles of calcium ions and L-arginine in synergistically promoting NO production. On the one hand, eNOS protein overexpressed after the transfection of peNOS in HUVECs. On the other hand, R(L)-CaP carrier generated calcium ions and L-arginine in lysosome, which can enhance the activity of eNOS. Based on biological mechanisms of intracellular NO production, this work designed a "one-stone-three-birds" strategy and prepared calcium ions and L-arginine-based bioactive carrier for the delivery of peNOS, in order to maximize the active NO output from VECs. In vitro cell migration and tube formation assays showed that HUVECs exposed to R(L)-CaP/peNOS possessed the highest number of migrated cells and tube formation (Figure 5C and D). Additionally, R(L)-CaP/peNOS group exhibited the lowest pro-inflammatory cytokines (IL-6 and TNF-α) (Figure 5E and F). These results suggested that R(L)-CaP/peNOS had the strongest pro-angiogenic effect and anti-inflammatory effect, benefiting to the synergistically amplified NO release. Furthermore, these results were verified in a hindlimb ischemic model in vivo, which further confirmed the synergistic effect of calcium ions, L-arginine and eNOS expression on NO production (Figure 6). In summary, we believe that the ternary synergistic gene delivery system R(L)-CaP/peNOS is promising for amplifying NO production via efficiently accelerating angiogenesis and alleviating inflammation.

Conclusion

In this work, a ternary synergistic gene delivery system R(L)-CaP/peNOS was ingeniously designed and developed to amply NO output in multiple directions. L-arginine modification augmented the transfection efficiency of CaP/peNOS to elevate the eNOS expression, and then served as NO substrate catalyzed by eNOS. At the same time, calcium ions produced by degradation of CaP carriers enhanced the activity of eNOS. In vitro experiments, the loading capability and transfection performance of R(L)-CaP and R(D)-CaP were confirmed to be superior to that of CaP. Additionally, HUVECs treated with R(L)-CaP/peNOS showed the strongest NO release, cell migration, tube formation and the lowest inflammatory levels compared to the CaP/peNOS and R(D)-CaP/peNOS groups. We also demonstrated the advantages of R(L)-CaP/peNOS in increasing blood reperfusion in hindlimb ischemia mice by accelerating angiogenesis and reducing inflammation, which can be attributed to the highest eNOS-derived NO production. Taking together, the combination strategy of peNOS transfection, L-arginine supplement and calcium ions addition is a promising therapeutic approach for certain vascular diseases, based on the synergistic NO production.

Animal Ethics Statement

Twenty 7-week-old male BALB/c mice were provided by the Animal Center of Qingdao University. The study in vivo was performed under protocols approved by the Animal Management Rules of the Ministry of Health of the People's Republic of China (document no. 55, 2001) and the examination and approval of the Experimental Animal Welfare Ethics Committee of The Affiliated Hospital of Qingdao University (ethical approval number: AHQU-MAL 20210110).

Acknowledgments

This study was supported by the Natural Science Foundation of Shandong Province (ZR2021MH354), the National Natural Science Foundation of China (81601591), and the Clinical Medicine + X Project of The Affiliated Hospital of Qingdao University (No. QDFY+X2021029).

Disclosure

The authors declare no conflicts of interest in this work.

References

1. Sun H-J, Wu Z-Y, Nie X-W, Bian J-S. Role of endothelial dysfunction in cardiovascular diseases: the link between inflammation and hydrogen sulfide. *Front Pharmacol*. 2020;10:1568. doi:10.3389/fphar.2019.01568
2. Mudau M, Genis A, Lochner A, Strijdom H. Endothelial dysfunction: the early predictor of atherosclerosis. *Cardiovasc J Afr*. 2012;23(4):222–231. doi:10.5830/CVJA-2011-068
3. Hu S, Li Z, Shen D, et al. Exosome-eluting stents for vascular healing after ischaemic injury. *Nat Biomed Eng*. 2021;5(10):1174–1188. doi:10.1038/s41551-021-00705-0
4. Marsico G, Martin-Saldana S, Pandit A. Therapeutic biomaterial approaches to alleviate chronic limb threatening ischemia. *Adv Sci*. 2021;8(7):2003119. doi:10.1002/advs.202003119
5. Wang X, Gao B, Suleiman GS, et al. A "controlled CO release" and "pro-angiogenic gene" dually engineered stimulus-responsive nanoplatform for collaborative ischemia therapy. *Chem Eng J*. 2021;424:130430. doi:10.1016/j.cej.2021.130430
6. Chen Y, Gao P, Huang L, et al. A tough nitric oxide-eluting hydrogel coating suppresses neointimal hyperplasia on vascular stent. *Nat Commun*. 2021;12(1):7079.
7. Janaszak-Jasiecka A, Siekierzycka A, Ploska A, Dobrucki IT, Kalinowski L. Endothelial dysfunction driven by hypoxia-the influence of oxygen deficiency on NO bioavailability. *Biomolecules*. 2021;11(7):982. doi:10.3390/biom11070982
8. Dash BC, Thomas D, Monaghan M, et al. An injectable elastin-based gene delivery platform for dose-dependent modulation of angiogenesis and inflammation for critical limb ischemia. *Biomaterials*. 2015;65:126–139. doi:10.1016/j.biomaterials.2015.06.037
9. Zhang K, Chen X, Li H, et al. A nitric oxide-releasing hydrogel for enhancing the therapeutic effects of mesenchymal stem cell therapy for hindlimb ischemia. *Acta Biomater*. 2020;113:289–304. doi:10.1016/j.actbio.2020.07.011
10. Yang T, Fruergaard AS, Winther AK, Zelikin AN, Chandrawati R. Zinc oxide particles catalytically generate nitric oxide from endogenous and exogenous prodrugs. *Small*. 2020;16(27):1906744. doi:10.1002/smll.201906744
11. Han C, Yu Q, Jiang J, et al. Bioenzyme-responsive l-arginine-based carbon dots: the replenishment of nitric oxide for nonpharmaceutical therapy. *Biomater Sci*. 2021;9(22):7432–7443. doi:10.1039/D1BM01184G
12. Burov ON, Kletskii ME, Kurbatov SV, Lisovin AV, Fedik NS. Mechanisms of nitric oxide generation in living systems. *Nitric Oxide-Biol Ch*. 2022;118:1–16. doi:10.1016/j.niox.2021.10.003
13. Kohli R, Meininger CJ, Haynes TE, Yan W, Self JT, Wu GY. Dietary L-arginine supplementation enhances endothelial nitric oxide synthesis in streptozotocin-induced diabetic rats. *J Nutr*. 2004;134(3):600–608. doi:10.1093/jn/134.3.600
14. Filippini A, D'Amore A, D'Alessio A. Calcium mobilization in endothelial cell functions. *Int J Mol Sci*. 2019;20(18):4525. doi:10.3390/ijms20184525
15. Mohan S, Harding L. Maintenance of cytosolic calcium is crucial to extend l-arginine therapeutic benefits during continuous dosing. *Nutr Res*. 2016;36(10):1114–1120. doi:10.1016/j.nutres.2016.07.002
16. Horinouchi T, Mazaki Y, Terada K, Miwa S. Extracellular Ca(2+) promotes nitric oxide production via Ca(2+)-sensing receptor-Gq/11 protein-endothelial nitric oxide synthase signaling in human vascular endothelial cells. *J Pharmacol Sci*. 2020;143(4):315–319. doi:10.1016/j.jphs.2019.06.009
17. Wang X, Su B, Gao B, et al. Cascaded bio-responsive delivery of eNOS gene and ZNF(580) gene to collaboratively treat hindlimb ischemia via pro-angiogenesis and anti-inflammation. *Biomater Sci*. 2020;8(23):6545–6560. doi:10.1039/D0BM01573C
18. Sun Y, Ma X, Jing X, Hu H, PAMAM-functionalized nanocrystals with needle-like morphology for effective cancer treatment. *Nanomaterials*. 2021;11(7):1640. doi:10.3390/nano11071640
19. Sokolova VV, Radtke I, Heumann R, Epple M. Effective transfection of cells with multi-shell calcium phosphate-DNA nanoparticles. *Biomaterials*. 2006;27(16):3147–3153. doi:10.1016/j.biomaterials.2005.12.030
20. Bisso S, Mura S, Castagner B, Couvreur P, Leroux J-C. Dual delivery of nucleic acids and PEGylated-bisphosphonates via calcium phosphate nanoparticles. *Adv Funct Mater*. 2019;142:142–152.
21. Huang X, Andina D, Ge J, Labarre A, Leroux J-C, Castagner B. Characterization of calcium phosphate nanoparticles based on a PEGylated chelator for gene delivery. *ACS Appl Mater Interfaces*. 2017;9(12):10435–10445. doi:10.1021/acsami.6b15925
22. Olton D, Li J, Wilson ME, et al. Nanostructured calcium phosphates (NanoCaPs) for non-viral gene delivery: influence of the synthesis parameters on transfection efficiency. *Biomaterials*. 2007;28(6):1267–1279. doi:10.1016/j.biomaterials.2006.10.026
23. Pedraza CE, Bassett DC, McKee MD, Nelea V, Gbureck U, Barralet JE. The importance of particle size and DNA condensation salt for calcium phosphate nanoparticle transfection. *Biomaterials*. 2008;29(23):3384–3392. doi:10.1016/j.biomaterials.2008.04.043
24. Hu J, Kovtun A, Tomaszewski A, et al. A new tool for the transfection of corneal endothelial cells: calcium phosphate nanoparticles. *Acta Biomater*. 2012;8(3):1156–1163. doi:10.1016/j.actbio.2011.09.013
25. Zhou Z, Li H, Wang K, et al. Bioreducible cross-linked hyaluronic acid/calcium phosphate hybrid nanoparticles for specific delivery of siRNA in melanoma tumor therapy. *ACS Appl Mater Interfaces*. 2017;9(17):14576–14589. doi:10.1021/acsami.6b15347
26. Liu Y, Wang T, He F, et al. An efficient calcium phosphate nanoparticle-based nonviral vector for gene delivery. *Int J Nanomed*. 2011;6:721–727. doi:10.2147/IJN.S17096

27. Ul Ain Q, Chung H, Chung JY, Choi JH, Kim YH. Amelioration of atherosclerotic inflammation and plaques via endothelial adrenoceptor-targeted eNOS gene delivery using redox-sensitive polymer bearing l-arginine. *J Controlled Release*. 2017;262:72–86. doi:10.1016/j.jconrel.2017.07.019
28. Zhou J, Wali ARM, Ma S, et al. Tailoring the supramolecular structure of guanidinylated pullulan toward enhanced genetic photodynamic therapy. *Biomacromolecules*. 2018;19(6):2214–2226. doi:10.1021/acs.biomac.8b00273
29. Yu J, Zhang J, Xing H, et al. Novel guanidinylated bioresponsive poly(amidoamine)s designed for short hairpin RNA delivery. *Int J Nanomed*. 2016;11:6651–6666. doi:10.2147/IJN.S115773
30. Zhang Y, Chu T, Sun L, et al. Study on the transfection efficiency of chitosan-based gene vectors modified with poly-l-arginine peptides. *J Biomed Mater Res A*. 2020;108(12):2409–2420. doi:10.1002/jbm.a.36992
31. Zavradashvili N, Memanishvili T, Kupatadze N, et al. Cell compatible arginine containing cationic polymer: one-pot synthesis and preliminary biological assessment. In: Adhikari R, Thapa S, editors. *Infectious Diseases and Nanomedicine I*. New Delhi: Springer; 2014:59–73.